



Inhibited coupling guiding hollow fibers for label-free DNA detection

F. GIOVANARDI,^{1,*} A. CUCINOTTA,² AND LUCA VINCETTI¹

¹Department of Engineering "Enzo Ferrari", University of Modena and Reggio Emilia, via Vivarelli 10, 41124 Modena, Italy

²Department of Engineering and Architecture, University of Parma, Parco Area delle Scienze, 181/A, 43124 Parma, Italy

*fabio.giovanardi@unimore.it

Abstract: The potentialities in using hollow core tube lattice fibers based on inhibited coupling wave-guiding for label-free DNA detection are numerically investigated and discussed here. The proposed sensing approach does not require any additional transducer component such as Bragg gratings, amplifying techniques such as nanoparticles nor coherent sources. It simply consists of the measurement of the transmittance of a piece of fiber some ten centimeters long. In case of matching DNA sequence, an additional bio-layer is laid down the dielectric-air interface causing a red shift of the transmission spectrum of the fiber. Results show a spectral sensitivity on the bio-layer with shift as high as 42 nm for every 10 nm of bio-layer and robustness against imperfect fiber coupling. The proposed approach can be easily applied to sensing of other complex molecular structures where the presence/absence of analyte can generate or not an additional layer.

© 2017 Optical Society of America

OCIS codes: (060.2370) Fiber optics sensors; (280.1415) Biological sensing and sensors; (060.4005) Microstructured fibers.

References and links

1. M. Barozzi, A. Manicardi, A. Vannucci, A. Candiani, M. Sozzi, M. Konstantaki, S. Pissadakis, R. Corradini, S. Selleri and A. Cucinotta, "Optical Fiber Sensors for Label-free DNA Detection," *J. Lightw. Technol.* **35**(16), 3461–3472 (2017).
2. Y. Huang, Z. Tian, L. Sun, D. Sun, J. Li, Y. Ran, and B. Guan, "High-sensitivity DNA biosensor based on optical fiber taper interferometer coated with conjugated polymer tentacle," *Opt. Express* **23**(21), 26962–26968 (2015).
3. A. Candiani, M. Sozzi, A. Cucinotta, S. Selleri, R. Veneziano, R. Corradini, R. Marchelli, P. Childs, and S. Pissadakis, "Optical Fiber Ring Cavity Sensor for Label-Free DNA Detection," *IEEE J. Sel. Top. Quantum Electron.* **18**(3), 1176–1183 (2012).
4. A. Bertucci, A. Manicardi, A. Candiani, S. Giannetti, A. Cucinotta, G. Spoto, M. Konstantaki, S. Pissadakis, S. Selleri, and R. Corradini, "Detection of unamplified genomic DNA by a PNA-based microstructured optical fiber (MOF) Bragg-grating optofluidic system," *Biosens. Bioelectron.* **63**, 248–254 (2015).
5. J. B. Jensen, G. Emilianov, O. Bang, P. E. Hoiby, L. H. Pedersen, T. P. Hansen, K. Nielsen, and A. Bjarklev, "Microstructured Polymer Optical Fiber Biosensors for Detection of DNA and Antibodies," in *Optical Fiber Sensors p. ThA2* (2006).
6. E. Coscelli, M. Sozzi, F. Poli, D. Passaro, a. Cucinotta, S. Selleri, R. Corradini, and R. Marchelli, "Toward A Highly Specific DNA Biosensor: PNA-Modified Suspended-Core Photonic Crystal Fibers," *IEEE J. Sel. Top. Quantum Electron.* **16**(4), 1–6 (2010).
7. D. Passaro, M. Foroni, F. Poli, A. Cucinotta, S. Selleri, J. Laegsgaard, and A. Bjarklev, "All-Silica hollow-core Microstructured Bragg Fibers for Biosensor Application," *IEEE Sensors Journal* **8**(7), 1280–1286 (2008).
8. F. Couny, F. Benabid, P. J. Roberts, P. S. Light, and M. G. Raymer, "Generation and photonic guidance of multi-octave optical-frequency combs," *Science* **318**(5853), 1118–1121 (2007).
9. B. Debord, M. Alharbi, T. Bradley, C. Fourcade-Dutin, Y. Y. Wang, L. Vincetti, F. Gérôme, and F. Benabid, "Hypocycloid-shaped hollow-core photonic crystal fiber, part I: arc curvature effect on confinement loss," *Opt. Express* **21**(23), 28597–28608 (2013).
10. B. Debord, A. Amsanpally, M. Chafer, A. Baz, M. Maurel, J. M. Blondy, E. Hugonnot, F. Scol, L. Vincetti, F. Gérôme, and F. Benabid, "Ultralow transmission loss in inhibited-coupling guiding hollow fibers," *Optica* **4**(2), 209–217 (2017).
11. N. V. Wheeler, T. D. Bradley, J. R. Hayes, M. A. Gouveia, Y. Chen, S. R. Sandoghchi, F. Poletti, M. N. Petrovich and D. J. Richardson, "Low Loss Kagome Fiber in the 1 μ m Wavelength Region," in *Advanced Photonics 2016 (IPR, NOMA, Sensors, Networks, SPPCom, SOF)*, OSA Technical Digest SoM3F.2 (2016).

12. L. Vincetti and V. Setti, "Waveguiding mechanism in tube lattice fibers," *Opt. Express* **18**(22), 23133–23146 (2010).
13. A. K. Mudraboyina, and J. Sabarinathan, "Protein Binding Detection Using On-Chip Silicon Gratings," *Sensors* **11**(12), 11295–11304 (2011).
14. L. Vincetti, "Empirical formulas for calculating loss in hollow core tube lattice fibers," *Opt. Express* **18**(10), 260459 (2016).
15. J. R. Hayes, S. R. Sandoghchi, T. D. Bradley, Z. Liu, R. Slavík, M. A. Gouveia, N. V. Wheeler, G. Jasion, Y. Chen, E. N. Fokoua, M. N. Petrovich, D. J. Richardson, and F. Poletti, "Antiresonant Hollow Core Fiber With an Octave Spanning Bandwidth for Short Haul Data Communications," *J. Lightw. Technol.* **35**(3), 437–442 (2017).
16. A. N. Kolyadin, A. F. Kosolapov, A. D. Pryamikov, A. S. Biriukov, V. G. Plotnichenko, and E. M. Dianov, "Light transmission in negative curvature hollow core fiber in extremely high material loss region," *Opt. Express* **21**(18), 9514–9519 (2013).
17. P. Uebel, M. Günendi, M. Frosz, G. Ahmed, N. Edavalath, J. Ménard, and P. Russell, "Broadband robustly single-mode hollow-core PCF by resonant filtering of higher-order modes," *Opt. Lett.* **41**(9), 1961–1964 (2016).

1. Introduction

The detection of specific DNA sequences in a cost-effective and sensitive way for environmental, biomedical, forensic, and food analysis is becoming a reality thanks to the development of lab on fiber platforms. Label-free sensors allow the direct sensing of the target DNA without the introduction of the marker. Usually, they exploit the molecular interactions between a surface and the DNA target sequence resulting in a generation of a biological layer. By monitoring the variations of the fiber transmission properties due to the bio-layer it is possible to detect the presence and concentration of particular DNA sequences [1]. In a standard optical fiber, the bio-layer can only be deposited on the outer surface of the cladding. This reduces sensitivity, requires either strong fiber tapering [2] or tilted period Bragg gratings, and the removal of polymeric coating making the bare fiber rigid and fragile [3]. Photonic Crystal Fibers (PCFs) represent a promising platform for overcoming limits of standard optical fibers and for developing cost-effective and sensitive sensors for the detection of specific DNA sequences [1]. The air holes running along the fiber length allow the infiltration of biologically active substances close to the core. So far, Solid Core (SC) and Hollow Core (HC) Photonic Band Gap (PBG) PCFs have been numerically and experimentally investigated for this purpose [4–7]. SC-PCFs are normally preferred because of their low loss over a broad wavelength range. Unfortunately, they suffer from a weak interaction between light and biological layer, as the interaction occurs through the evanescent tail of the propagating mode. Consequently, techniques to enhance this interaction, such as nanoparticles, must be used [4]. In addition in SC-PCFs bio-layers only modify the mode effective index. Fiber Bragg Gratings (FBGs) must be thus introduced in the PCF to transduce the phase variation into amplitude variation easily detectable [4]. Finally, since FBGs are narrow band components the detection analysis can be done only on very narrow wavelength ranges. HC-PCFs based on Photonic Band Gap confinement guarantee a stronger interaction since the bio-layer is in the fiber core region. Unfortunately, they suffer from a narrow bandwidth and the Bragg grating inscription is very hard. Moreover, the micro-metric scale hole size composing the cladding makes the fiber-liquid filling time-consuming. Inhibited Coupling (IC) Fibers are a new kind of HC-PCFs [8]. The particular micro-structured cladding guarantees the inhibition of coupling between core modes and cladding modes over wide wavelength ranges [9]. This results in a transmission spectrum composed by an alternation of high and low loss regions. The introduction of hypocycloid core contour has led to HC-IC-PCFs with an octave bandwidth and propagation loss as low as tens of dB/km, both in near-infrared and visible spectral regions [10, 11]. The spectral collocation of the high loss regions depends on the thickness of dielectric struts composing the microstructured cladding [12]. This property can be fruitfully exploited for label-free DNA sensing. Since thickness is affected by bio-layer, the high loss spectral regions are directly modulated by the bio-layer allowing avoiding the use of Bragg gratings or other transduction components. In addition, the very thin struts (hundreds of nm) [9–11] make the shift extremely sensitive also to a very thin bio-layer. Finally, the larger

pitch with respect to HC-PBG-PCFs allows a better infiltration of the analyte inside the core and surrounding holes. In this work, through a numerical investigation, we propose a label-free DNA sensor based on the measurement of transmission loss of HC-IC-PCFs. In particular, we consider a Tube Lattice Fiber (TLF) in which the microstructured cladding simply consists in a number of dielectric tubes surrounding a hollow core [10, 12, 15, 16]. Compare to IC Kagome fibers, in TLFs a hypocycloid core contour can be obtained with nontouching tubes. The complete absence of any connecting nodes in the core contour strongly favors IC [10, 16]. The sensing mechanism simply consists on the measurement of the transmittance of a piece of TLF some tens of centimeters long. Since it is based on attenuation measurement, both coherent and incoherent sources can be used. Results confirm a shift of the transmittance spectrum proportional to the layer thickness with a sensitivity of 42 nm for each 10 nm of bio-layer thickness. This is orders of magnitude higher than those obtained with SC-PCFs combined with Bragg gratings.

2. Principle of operation

The label-free selective detection of DNA strands can be obtained by using probes of Peptide Nucleic Acids (PNAs) attached to a silica surface through covalent link as shown in Fig. 1(a). PNA binds very effectively with DNA sequence to detect. Details of the technique and surface treatment can be found in [1] and [6]. After this process called functionalization, a solution containing the DNA to analyze is infiltrated inside the fiber and then removed. If the analyzed solution contains the DNA sequence to detect, several long DNA strands will be found on the surface, bound with the complementary PNA [Fig. 1(b)]. They can be effectively modeled as an additional layer (bio-layer) having thickness t_{ly} and refractive index n_{ly} [Fig. 1(c) [4]. Figure 2(a) shows the cross-section of the fiber under investigation. It consists of a TLF where

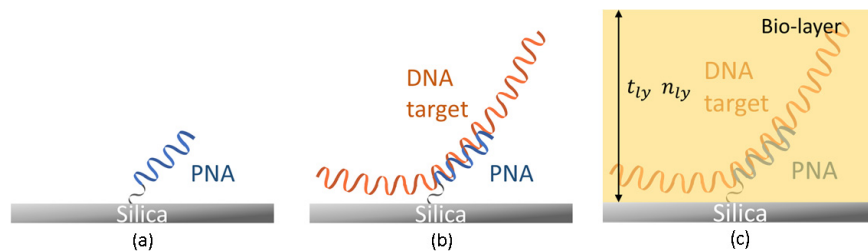


Fig. 1. (a) PNA linked to silica surface with a covalent bond. (b) DNA strand containing the sequence to detect bounded with PNA. (c) DNA strands modeled as a layer with thickness t_{ly} and refractive index n_{ly} .

the cladding is composed by a regular arrangement of silica tubes with external radius r_{ext} , thickness t_{si} , and spaced by δ . In the present analysis, the number of tubes is fixed to eight. Figures. 2(b)-2(e) show the intensity profile of the fiber modes: core modes, cladding modes, and hole modes respectively. In TLFs, core modes are well confined inside the hollow core and the value of the light intensity on and inside the dielectric membrane composing the tubes is extremely low [10, 14]. Cladding modes are confined inside the dielectrics and light intensity is quite strong both inside and on the dielectric tube membranes. Finally, hole modes are mainly confined inside the tube holes. Since they are not involved in the sensing mechanism hereinafter they will be not considered in the discussion. Due to the coupling between core modes and cladding modes, the spectrum of the propagation loss consists in an alternation of high and low loss regions corresponding to the resonance condition (same effective index) between core modes and cladding modes having slow [Fig. 2(d)] and quick [Fig. 2(c)] spatial variation along the tube membranes respectively. The spectral position of the high loss regions can be well

estimated by the cut-off wavelength of the $HE_{\nu,1}$ modes of the single tube fiber [12, 14]:

$$\lambda_m = \frac{2t_{si}}{m} \sqrt{n_{si}^2 - 1}, \quad (1)$$

being t_{si} , and n_{si} the silica thickness and refractive index respectively, $m = \nu - 1$ and ν the mode radial number. An example of propagation loss spectrum for a TLF with $t_{si} = 700nm$,

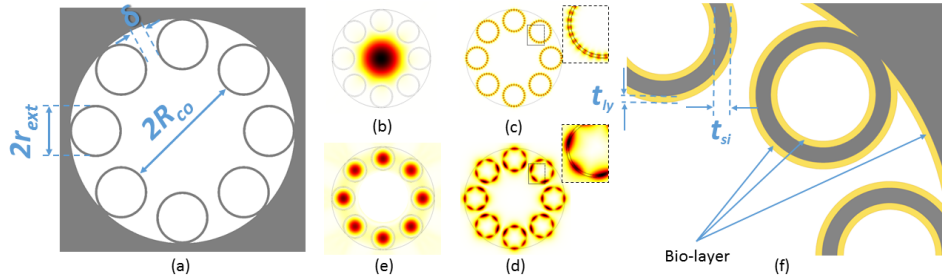


Fig. 2. (a) Tube Lattice Fiber cross-section. (b) core mode (c),(d) cladding modes with quick and slow spatial dependence respectively. (e) hole mode. (f) detail of a fiber's tubes with bio-layer.

$r_{ext} = 8.5\mu m$, $R_{co} = 20.5\mu m$, and n_{si} is shown in Fig. 3. Here for sake of simplicity only the confinement loss (CL) of the fundamental mode (FM) has been considered. Actually, in TLFs there is more than one loss source affecting propagation loss, in particular for short wavelengths [10]. However they exhibit a wavelength dependence very similar to CL, that is an alternation of low and high loss defined by Eq. (1) [10, 14], so the operation principle of the sensor is not compromised by other loss sources. In case of presence of the right DNA sequence on silica surfaces, an additional bio-layer is present [Fig. 2(f)]. The thicker tubes cause a red shift of the high loss regions according to Eq. (1) as shown in Fig. 3. The shift depends on thickness and refractive index of the bio-layer. Recently, the refractive index of a biological layer has been estimated to be $n_{ly} = 1.5$ [13]. Since n_{ly} is quite close to the silica refractive index in the visible and near infrared spectral region, the multilayer tubes can be approximated with homogeneous tubes having thickness $t_{eq} = t_{si} + 2t_{ly}$ and refractive index n_{si} . With this assumption, the spectral sensitivity of the high loss regions to bio-layer thickness variation $S_{\lambda, t_{ly}}$ can be easily derived from Eq. (1):

$$S_{\lambda, t_{ly}} = \frac{d\lambda}{t_{ly}} = \frac{4}{m} \sqrt{n_{si}^2 - 1}, \quad (2)$$

being $d\lambda$ the spectral shift and $t_{ly} = dt/2$ a half of the thickness variation. With $t_{si} = 700nm$, and $n_{si} = 1.45$ the estimated sensitivity is $S_{\lambda, t_{ly}} = \frac{4.2}{m} nm/nm$, that is $126/m nm$ of spectral shift each $30 nm$ of bio-layer. That sensitivity is confirmed by numerical results reported in Fig. 3. The red shift of the high loss regions is about $140 nm$ for the first ($m = 1$) peak, $70 nm$ for the second one ($m = 2$), and $46 nm$ for the third one ($m = 3$). This strong sensitivity with respect to other approaches is due to the completely different mechanism the proposed sensor is based on. In the previous approaches, the bio-layer affects the effective index of the core modes of the fiber. In the proposed fibers, bio-layer affects the parameters of the cladding modes. The influence on the core modes is negligible due to the low value of their intensity in and around tube membranes. On the contrary cladding modes are well confined inside the silica and they strongly depend on refractive index and thickness of the material composing the tube. The sensing is thus based on the strong changing of the cladding modes properties and not on the weak changing of the core modes. In addition, the coupling between core and cladding modes and the consequent variation of the propagation loss are inherent in the waveguiding mechanism.

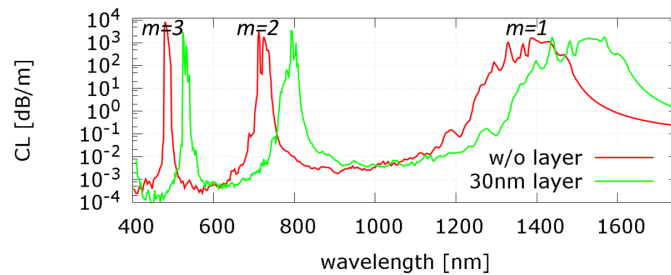


Fig. 3. FM confinement loss of the analyzed fiber without bio-layer (red line) and with 30 nm of bio-layer (green line).

Thanks to that, a spectral variation of the transmitted power depending on presence/absence of bio-layers can be obtained without adding any other transducer component or interferometric techniques.

3. Detection scheme and numerical results

Figure 4 shows the schematic of the sensor. Thanks to the waveguiding properties of the fiber, the sensor can be simply composed of a piece of fiber with length L , a broadband light source and a spectrum analyzer. Both coherent and incoherent sources can be used. Figure 5 shows

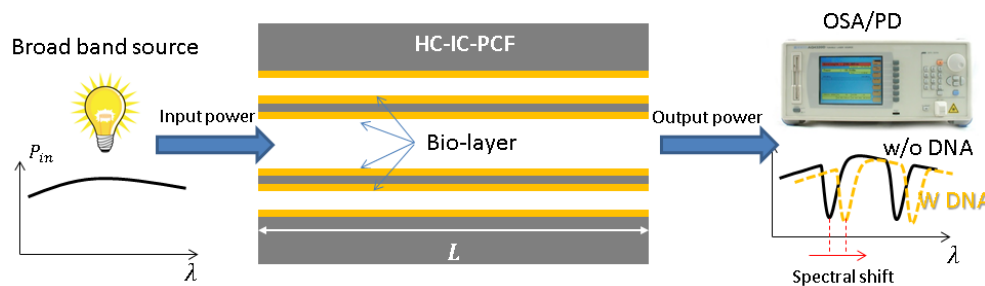


Fig. 4. Schematic of the optical set-up. A broadband coherent or incoherent source is coupled at one end of the fiber. The transmitted light is collected from the other end and its spectrum is analyzed. The presence or absence of a spectral shift correspond to presence or absence of the DNA sequence searched for respectively.

the simulated transmittance $T = P_{out}/P_{in} = CL \cdot L$ of the analyzed TLF with $L = 20$ cm, without and with three different bio-layer thicknesses. The chosen thickness guarantees the red edge of the first high loss region ($m = 1$) and thus of the transmittance dip, is close to telecom band $1500\text{nm} - 1600\text{nm}$ where inexpensive and reliable components can be easily found. The total volume to be infiltrated in the hollow fiber is about $0.55 \mu\text{l}$. The blue edges of the dips are less sharp and smooth than the red one because of the residual coupling between core mode and cladding modes with slow spatial dependence [12, 14]. By focusing on red edges, the spectral shift is about 47 nm every 10 nm of bio-layer thickness at -10 dB of transmittance. This sensitivity is two orders of magnitude higher than the one obtained with SC-PCF with a Bragg grating inscribed [4]. Figure 5 also shows the spectral shift in case of lower refractive index of the bio-layer. By considering the worst case on $n_{ly} = 1.3$ and $t_{ly} = 10$ nm the spectral shift is about 30 nm. TLFs are multimode fibers. Though high order modes (HOMs) can be filtered out with a proper design of the tubes [12, 17], here we considered a TLFs without HOMs suppression. HOMs are excited in case of imperfect coupling between source and fiber. Here we

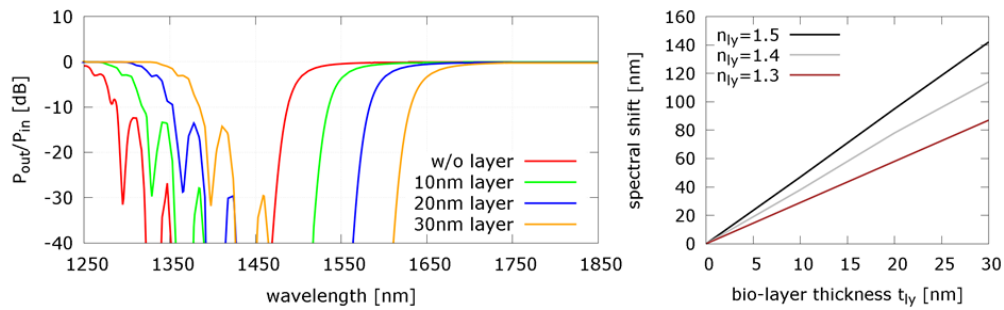


Fig. 5. Left: Transmission spectrum of the analyzed fiber without bio-layer and with different bio-layer thickness (10nm, 20nm, 30nm). Only FM propagation is assumed. Right: Spectral shift vs bio-layer thickness for different values of n_{ly} .

investigate the effect on sensor performance of multimode propagation due to imperfect fiber excitation. Both wrong spot size and axis misalignment have been analyzed. Sixteen different conditions of excitation have been considered by changing the spot size from $10 \mu\text{m}$ to $30 \mu\text{m}$ and the axis misalignment from 0 to $0.75R_{co}$ in steps of $0.25R_{co}$. Figure 6 shows the transmittance of the sixteen conditions with and without a very thin bio-layer of 10 nm . Despite the alteration of the transmittance spectrum and the very thin bio-layer considered, the two bundles of curves are well separated and the red shift due to bio-layer is still clear. This robustness is because the high loss regions of HOMs are also governed by Eq. (1).

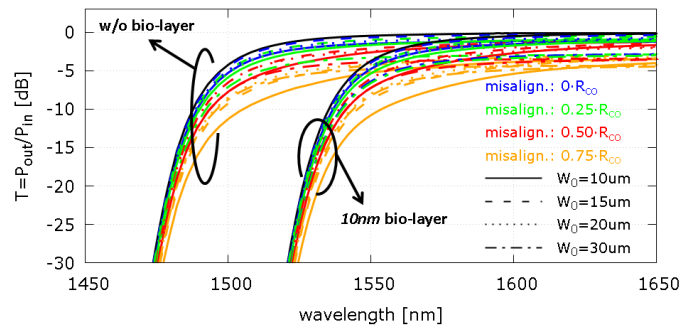


Fig. 6. Transmission spectrum of the analyzed fiber with and without 10 nm bio-layer for different excitation conditions obtained by changing both spot size (different line style) and alignment (different color) of a input gaussian beam.

4. Conclusion

In this paper a label-free DNA sensor based on Tube Lattice Fiber has been proposed and numerically investigated. Thanks to the waveguiding mechanism based on Inhibited Coupling the sensor does not require additional transducer components such as Bragg gratings or nanoparticles to enhance the sensitivity. The sensor is simply based on the measurement of the fiber transmission loss and does not require a coherent source. Numerical results show a spectral shift of 42 nm with bio-layer having refractive index 1.5 and thickness 10 nm . Such sensitivity is about two orders of magnitude higher than DNA sensors based on solid core PCFs with Bragg grating and nanoparticles. The proposed approach can be easily applied to other sensing layouts where the presence/absence of analyte can generate or not an additional layer.